Impaired functional communication between the L-type calcium channel and mitochondria contributes to metabolic inhibition in the *mdx* heart

Helena M. Viola[a], Abbie M. Adams[b], Stefan M. K. Davies[c], Susan Fletcher[b,d], Aleksandra Filipovska[c], and Livia C. Hool[a,e,1]

[a]School of Anatomy, Physiology and Human Biology, The University of Western Australia, Crawley, WA 6009, Australia; [b]Western Australian Neuroscience Research Institute and Centre for Neuromuscular and Neurological Disorders, The University of Western Australia, QEII Medical Centre, Nedlands, WA 6009, Australia; [c]Harry Perkins Institute for Medical Research, The University of Western Australia, Perth, WA 6000, Australia; [d]Centre for Comparative Genomics, Murdoch University, Murdoch, WA 6150, Australia; and [e]Victor Chang Cardiac Research Institute, Darlinghurst, NSW 2010, Australia

Duchenne muscular dystrophy is a fatal X-linked disease characterized by the absence of dystrophin. Approximately 20% of boys will die of dilated cardiomyopathy that is associated with cytoskeletal protein disarray, contractile dysfunction, and reduced energy production. However, the mechanisms for altered energy metabolism are not yet fully clarified. Calcium influx through the L-type Ca^{2+} channel is critical for maintaining cardiac excitation and contraction. The L-type Ca^{2+} channel also regulates mitochondrial function and metabolic activity via transmission of movement of the auxiliary beta subunit through intermediate filament proteins. Here, we find that activation of the L-type Ca^{2+} channel is unable to induce increases in mitochondrial membrane potential and metabolic activity in intact cardiac myocytes from the murine model of Duchenne muscular dystrophy (*mdx*) despite robust increases recorded in *wt* myocytes. Treatment of *mdx* mice with morpholino oligomers to induce exon skipping of dystrophin exon 23 (that results in functional dystrophin accumulation) or application of a peptide that resulted in block of voltage-dependent anion channel (VDAC) "rescued" mitochondrial membrane potential and metabolic activity in mdx myocytes. The mitochondrial VDAC coimmunoprecipitated with the L-type Ca^{2+} channel. We conclude that the absence of dystrophin in the *mdx* ventricular myocyte leads to impaired functional communication between the L-type Ca^{2+} channel and mitochondrial VDAC. This appears to contribute to metabolic inhibition. These findings provide new mechanistic and functional insight into cardiomyopathy associated with Duchenne muscular dystrophy.

ion channels | structure | cytoskeleton

Duchenne muscular dystrophy affects 1:3,500 males, and in addition to skeletal muscle damage and atrophy, boys also develop a dilated cardiomyopathy due to the absence of expression of dystrophin. This pathology involves myocyte remodelling, disorganization of cytoskeletal proteins, and contractile dysfunction (1, 2). Early metabolic and signaling alterations have been reported in 10- to 12-wk-old murine model of Duchenne muscular dystrophy (*mdx*) hearts before the development of overt contractile dysfunction (2). However, the mechanisms by which absence of dystrophin leads to mitochondrial dysfunction and compromised cardiac function in *mdx* hearts are not fully clarified yet.

Cytoskeletal proteins stabilize cell structure. In mature muscle, intermediate filaments form a 3D scaffold that extend from the Z disks to the plasma membrane and traverse cellular organelles such as t-tubules, sarcoplasmic reticulum, and mitochondria (3). Intermediate filaments and microtubules interact directly with mitochondria by binding to outer mitochondrial membrane proteins. In addition to a physical association, cytoskeletal proteins also regulate the function of proteins in the plasma membrane and within the cell (4). The L-type Ca^{2+} channel (I_{Ca-L}) or dihydropyridine receptor (DHPR) is anchored to F-actin networks by subsarcolemmal stabilizing proteins that also tightly regulate the function of the channel (5–7). Disruption of actin filaments significantly alters I_{Ca-L} current (5, 7, 8).

Calcium influx through I_{Ca-L} is a requirement for contraction. I_{Ca-L} can also regulate mitochondrial function. Activation of I_{Ca-L} with application of the DHPR agonist BayK(-) or voltage clamp of the plasma membrane can influence mitochondrial superoxide production, NADH production, and metabolic activity in a calcium-dependent manner (9, 10). Activation of I_{Ca-L} can also increase mitochondrial membrane potential (Ψ_m) in a calcium-independent manner (9). The response is reversible upon inactivation of I_{Ca-L}. The response also depends on actin filaments because depolymerization of actin prevents the increase in Ψ_m (9). Similarly preventing movement of the beta auxiliary subunit of I_{Ca-L} with application of a peptide derived against the alpha-interacting domain of the channel attenuates the increase in Ψ_m (9). Therefore, we have proposed that I_{Ca-L} influences metabolic activity through transmission of movement of the channel via cytoskeletal proteins. Here, we sought to identify whether cytoskeletal disruption due to the absence of dystrophin leads to mitochondrial dysfunction and compromised cardiac function in *mdx* hearts. Specifically, we investigated whether the absence of dystrophin in ventricular

Significance

Duchenne muscular dystrophy (DMD) is a fatal X-linked disease that results in cardiomyopathy and heart failure. The cardiomyopathy is characterized by cytoskeletal protein disarray, contractile dysfunction, and reduced energy production. The mechanisms for altered energy metabolism are not yet fully clarified. The L-type Ca^{2+} channel regulates excitation and contraction in the heart, and can regulate mitochondrial function via the movement of cytoskeletal proteins. Here, we find that myocytes from the murine model of DMD (*mdx*) exhibit impaired communication between the L-type Ca^{2+} channel and the mitochondria that results in poor energy production. Morpholino oligomer therapy targeting dystrophin or block of the mitochondrial voltage-dependent anion channel (VDAC) "rescues" metabolic function, indicating that impaired communication between the L-type Ca^{2+} channel and VDAC contributes to the cardiomyopathy.

www.manaraa.com

myocytes from *mdx* mice results in impaired communication between I_{Ca-L} and mitochondria and, subsequently, metabolic inhibition.

Results

I_{Ca-L} Measured in mdx Myocytes Exhibit Altered Inactivation Kinetics.
We measured I_{Ca-L} currents in myocytes isolated from hearts of *mdx* mice and compared them with currents recorded from *wt* myocytes. Consistent with previous reports (11, 12) we find I_{Ca-L} current density in myocytes from 8-wk-old *wt* mice is not different from current density recorded in myocytes from 8-wk-old *mdx* mice (6.2 ± 0.8 pA/pF, *n* = 10 vs. 7.9 ± 1.6 pA/pF, *n* = 9; *P* = not significant). In addition, there was no difference in cell size between *mdx* and *wt* myocytes (12). Through immunoblotting, we confirm that channel expression is not altered in *mdx* myocytes (Fig. S1). However, in *mdx* myocytes, the inactivation of the

current was significantly slower (τ = 26.15 ± 1.75 vs. 21.06 ± 1.29 ms; Fig. 1 *A* and *B*). Consistent with a delayed inactivation rate, we have demonstrated that the inactivation integral of current and total integral of current are significantly greater in myocytes from *mdx* hearts compared with myocytes from *wt* hearts (12). Additionally, the activation integral of current in *mdx* and *wt* myocytes does not differ (12). The delayed inactivation of the current persists in the *mdx* myocyte when barium is used as a carrier (13). We cannot definitively state that alterations in intracellular calcium are not responsible for the response; however, these findings suggest that the delay in inactivation may occur as a result of alterations in cytoskeletal structure. Consistent with this argument and with previous reports, we find that immobilizing the beta subunit of I_{Ca-L} by exposing *wt* myocytes to a peptide derived against the alpha-interacting domain (AID) of
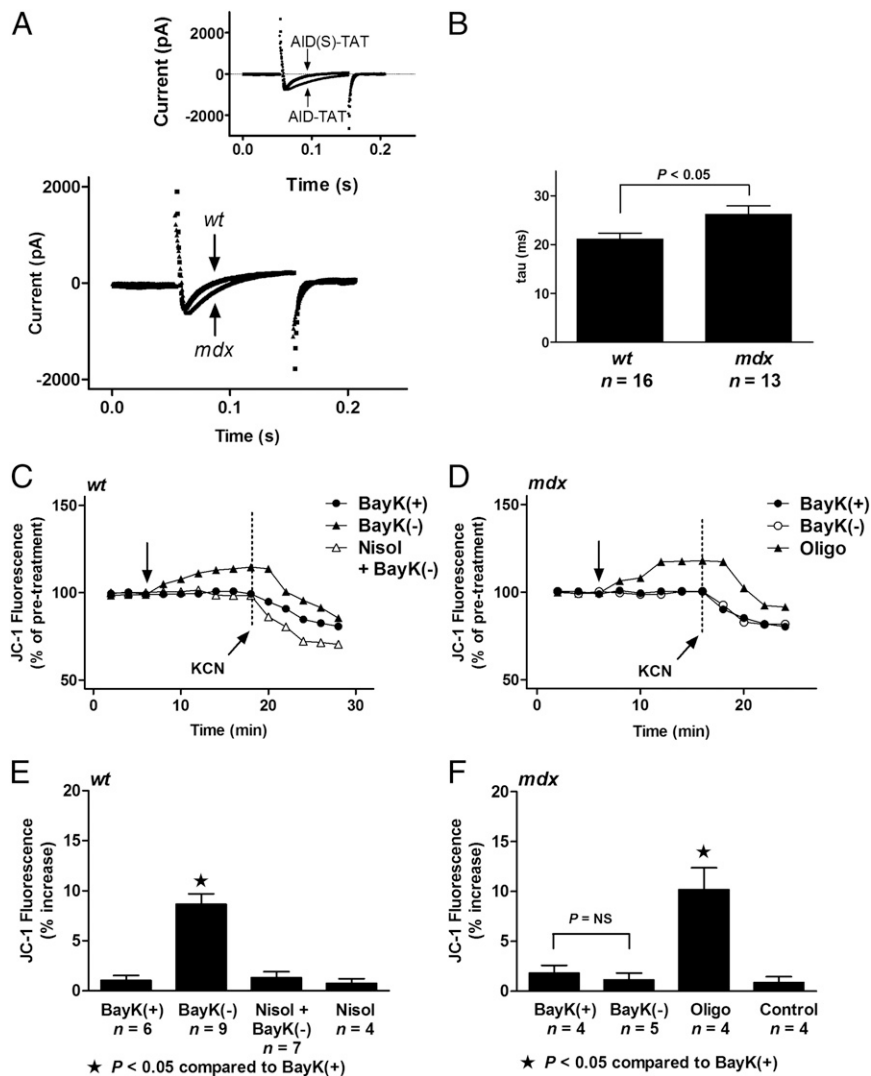

Fig. 1. Absence of dystrophin alters I_{Ca-L} current and Ψ_m in *mdx* myocytes. (*A*) I_{Ca-L} current traces recorded from a myocyte from a *mdx* heart and a myocyte from a *wt* heart as indicated. (*A, Inset*) I_{Ca-L} current traces from a *wt* myocyte (250 pF) exposed to a peptide derived against the alpha-interacting domain of I_{Ca-L} (AID-TAT, 1 μM) or a *wt* myocyte (220 pF) exposed to a scrambled control peptide [AID(S)-TAT, 1 μM] as indicated. Microelectrodes contained the following: 115 mM CsCl, 10 mM Hepes, 10 mM EGTA, 20 mM tetraethylammonium chloride, 5 mM MgATP, 0.1 mM Tris-GTP, 10 mM phosphocreatine, and 1 mM $CaCl_2$ (pH adjusted to 7.05 at 37 °C with CsOH). Currents were measured in extracellular modified Tyrode's solution containing the following: 140 mM NaCl, 5.4 mM CsCl, 2.5 mM $CaCl_2$, 0.5 mM $MgCl_2$, 5.5 mM Hepes, and 11 mM glucose (pH adjusted to 7.4 with NaOH). (*B*) Mean ± SEM of rate of inactivation (tau) for *mdx* myocytes and *wt* myocytes. (*C*–*F*) Direct activation of I_{Ca-L} results in an increase in Ψ_m in *wt* but not *mdx* myocytes. Representative ratiometric JC-1 fluorescence recorded from *wt* myocytes (*C*), and *mdx* myocytes (*D*), before and after exposure to 10 μM BayK(-) or 10 μM BayK(+). Vertical arrow indicates when drug was added. Four millimolar KCN was added to collapse Ψ_m as indicated. Mean ± SEM of increases in JC-1 fluorescence for all *wt* (*E*) and *mdx* (*F*) myocytes exposed to treatments as indicated. Nisol, 10 μM nisoldipine; Oligo, 20 μM oligomycin. Oligo alone induced a robust increase in JC-1 signal in *mdx* myocytes.

www.manaraa.com

I_{Ca-L} slows inactivation of the current (AID-TAT; Fig. 1 *A, Inset*) (6, 9, 10). Because the auxiliary beta subunit regulates inactivation of I_{Ca-L} current (14, 15), we propose that the alterations in I_{Ca-L} inactivation in the *mdx* myocyte result from disruption of the cytoskeleton due to the absence of dystrophin.

Direct Activation of I_{Ca-L} Increases Ψ_m in wt but Not mdx Myocytes. We have demonstrated that activation of I_{Ca-L} with application of DHPR agonist BayK(-) or voltage clamp of the plasma membrane results in an increase in Ψ_m in guinea-pig ventricular myocytes (9). BayK(-) increases I_{Ca-L} in the *mdx* myocyte (12). We examined whether the absence of dystrophin altered the increase in Ψ_m after application of Bay K(-) in myocytes from *mdx* mice. We performed experiments in quiescent ventricular myocytes with consistent ATP utilization because this approach allowed us to more readily explore the effects of I_{Ca-L} activation on mitochondrial function. Exposure of wild-type (*wt*) myocytes to BayK(-) increased Ψ_m measured as changes in JC-1 signal by 7.61 ± 1.04% compared with *wt* myocytes exposed to inactive enatiomer BayK(+) (Fig. 1 *C* and *E*). The response could be attenuated with application of I_{Ca-L} antagonist nisoldipine. However, in *mdx* myocytes, BayK(-) could not elicit an increase in JC-1 signal (Fig. 1 *D* and *F*). Myocytes from *mdx* hearts exhibited functional electron transport because the ATP synthase blocker oligomycin induced a significant increase in JC-1 signal (Fig. 1 *D* and *F*). To further confirm that the signal was measuring changes in Ψ_m, we induced a collapse of Ψ_m with application of potassium cyanide (KCN) (Fig. 1 *C* and *D*).

Alterations in Ψ_m After Activation of I_{Ca-L} Do Not Require Calcium. Mitochondrial membrane potential can function independent of changes in intracellular calcium in the range of 0–400 nM (16). We tested the effect of activation of I_{Ca-L} on Ψ_m in *wt* and *mdx* myocytes in calcium-free and EGTA-containing Hepes-buffered solution (HBS). Exposure of *wt* myocytes to BayK(-) increased Ψ_m measured as changes in JC-1 signal by 12.1 ± 1.4% compared with *wt* myocytes exposed to inactive enatiomer BayK(+) (Fig. 2 *A, i* and *D*). The response could be attenuated with application of I_{Ca-L} antagonist nisoldipine. In some experiments, *wt* myocytes were incubated in calcium-free EGTA containing HBS for at least 3 h and perfused intracellularly with 3 mM EGTA and 5 mM 1,2-bis(o-aminophenoxy)ethane-*N,N,N',N'*-tetraacetic acid (BAPTA) to deplete intracellular calcium stores. The *wt* myocytes exhibited similar increases in Ψ_m after activation of I_{Ca-L} (Fig. 2 *A, ii*). To further confirm whether calcium was involved in the response, *wt* myocytes that were incubated in calcium-free EGTA containing HBS for at least 3 h as described above were also exposed to caffeine (2 μM) that stimulates release of calcium from ryanodine receptors in the sarcoplasmic reticulum. There was no significant alteration in JC-1 signal after the addition of caffeine (Fig. 2 *C* and *D*). Exposure of *wt* myocytes to caffeine and BayK(-) resulted in an increase in JC-1 signal similar to that of BayK(-) alone (Fig. 2 *C* and *D*).

However, in *mdx* myocytes, BayK(-) could not elicit an increase in JC-1 signal (Fig. 2 *B* and *E*). The mitochondria in myocytes from *mdx* hearts exhibited functional electron transport because the ATP synthase blocker oligomycin induced a significant increase in JC-1 signal (Fig. 2*E*). These data confirm that the alteration in Ψ_m in response to BayK(-) does not depend on changes in intracellular calcium (9, 17). We propose that the loss of regulation of Ψ_m by I_{Ca-L} in the *mdx* myocyte results from disruption of the cytoskeleton due to the absence of dystrophin.

To determine whether the response depended on the presence of dystrophin, we injected *mdx* mice with 10 mg/kg per wk phosphorodiamidate morpholino oligomer (PMO) targeting mouse dystrophin exon 23 for 24 wk. This treatment induces removal of exon 23 during processing of the primary transcript and results in expression of a slightly shorter dystrophin protein (18). Similar

therapy is being administered to Duchenne muscular dystrophy patients in clinical trials with excellent results demonstrated as maintaining ambulation (19, 20). Uptake of the oligomers in mouse cardiac muscle can be detected as evidence of exon skipping on RT-PCR (Fig. 2 *F, i*), by the presence of dystrophin on immunoblot (Fig. 2 *F, ii*) and immunohistochemistry staining in cryosections (Fig. 2*G*). We find that BayK(-) can elicit a significant increase in JC-1 signal in myocytes isolated from hearts of *mdx* mice treated with PMOs, indicating that treatment with oligomers "rescued" the JC-1 response (Fig. 2 *B* and *E*). These data confirm that the alteration in Ψ_m in response to BayK(-) requires dystrophin.

Activation of I_{Ca-L} Increases Metabolic Activity in wt but Not mdx Myocytes. We examined whether activation of I_{Ca-L} altered metabolic activity in myocytes isolated from *mdx* hearts. Consistent with previous results (9), BayK(-) elicited a significant increase in metabolic activity (assessed as formation of formazan from tetrazolium salt) in myocytes from *wt* mice (Fig. 3 *A* and *B*). The response could be attenuated with application of nisoldipine or block of calcium uptake into the mitochondria (Ru360), but not with an inhibitor of the ryanodine receptor (dantrolene; Fig. 3*B*). However, in myocytes from *mdx* hearts, BayK(-) could not elicit an increase in metabolic activity (Fig. 3 *A* and *C*). Application of oligomycin caused a significant decrease in metabolic activity, indicating the cells were metabolically active (Fig. 3*C*).

We also examined changes in mitochondrial electron transport by measuring alterations in flavoprotein oxidation (as autofluorescence) in the myocytes in response to activation of I_{Ca-L}. In *wt* myocytes, BayK(-) caused a small but significant increase in flavoprotein oxidation that could be attenuated with application of nisoldipine (Fig. 3 *D* and *F*). However, BayK(-) could not elicit an increase in flavoprotein oxidation in *mdx* myocytes despite an increase recorded in response to application of carbonyl cyanide-*4*-(trifluoromethoxy)phenylhydrazone (FCCP) (Fig. 3 *E* and *G*). To determine whether the response depended on the presence of dystrophin, we examined the effect of BayK(-) on flavoprotein oxidation in myocytes isolated from hearts of PMO-treated *mdx* mice. We find that BayK(-) can elicit a significant increase in flavoprotein oxidation in myocytes isolated from hearts of PMO-treated *mdx* mice, indicating that treatment with oligomers partially rescued the response (Fig. 3 *E* and *G*). These data provide evidence that loss of regulation of metabolic activity by I_{Ca-L} in the *mdx* myocyte results from disruption of the cytoskeleton due to the absence of dystrophin.

I_{Ca-L} Associates with the Mitochondrial VDAC via Cytoskeletal Proteins. We have demonstrated that activation of I_{Ca-L} results in an increase in Ψ_m in guinea-pig ventricular myocytes, and the response depends on an intact cytoskeleton because disruption of F-actin filaments attenuated the increase in Ψ_m (9). We assessed alterations in Ψ_m in myocytes from *wt* mice treated with either latrunculin A to depolymerize F-actin filaments, or a peptide directed toward the AID of I_{Ca-L} (AID-TAT) to immobilize the auxiliary beta subunit of I_{Ca-L}. Myocytes treated with either latrunculin A or AID-TAT demonstrated attenuation of increased Ψ_m following exposure to BayK(-) (Fig. 4 *A* and *E*). These data suggest that the response depends on an intact cytoskeletal architecture.

Voltage-dependent anion channel (VDAC) resides in the outer mitochondrial membrane and associates with the adenine nucleotide translocator (ANT) that is located in the inner mitochondrial membrane (21). The VDAC/ANT complex is responsible for trafficking of ATP/ADP in and out of the mitochondria (22). Because Ψ_m depends on the function of the VDAC/ANT complex, we investigated whether I_{Ca-L} was associated with the outer mitochondrial membrane protein VDAC. We immunoprecipitated VDAC protein from hearts of 8-wk-old *wt* and *mdx* mice and immunoblotted the protein against an I_{Ca-L} antibody. We identified a band at ~220 kDa on immunoblot consistent with I_{Ca-L}

Viola et al.

www.manaraa.com

protein (Fig. 4 *B, i*). Conversely, when we immunoprecipitated I_{Ca-L} protein and probed the protein with anti-VDAC antibody, we identified a protein at 37 kDa, consistent with VDAC (Fig. 4 *B, i*). The immunoprecipitated I_{Ca-L} proteins from *wt* heart and *mdx* heart were analyzed by mass spectrometry on a Velos Orbitrap (Tables S1–S4). A number of similar proteins were identified in immunoprecipitated protein from *wt* heart and *mdx* heart,

including the α_{1C} pore forming and auxiliary beta subunits of I_{Ca-L}. Known regulators of I_{Ca-L} function were identified, including β-tubulin, Ca^{2+}/calmodulin-dependent protein kinase II (CaMKII), and A-kinase anchor protein (AKAP) (23–25) (Fig. 4 *B, ii*). Proteins that were identified in *wt* hearts and not *mdx* hearts, and proteins identified in *mdx* hearts but not *wt* hearts, are listed in Table S4. Consistent with our in vitro data (Fig. 4 *A* and *E*), F-actin
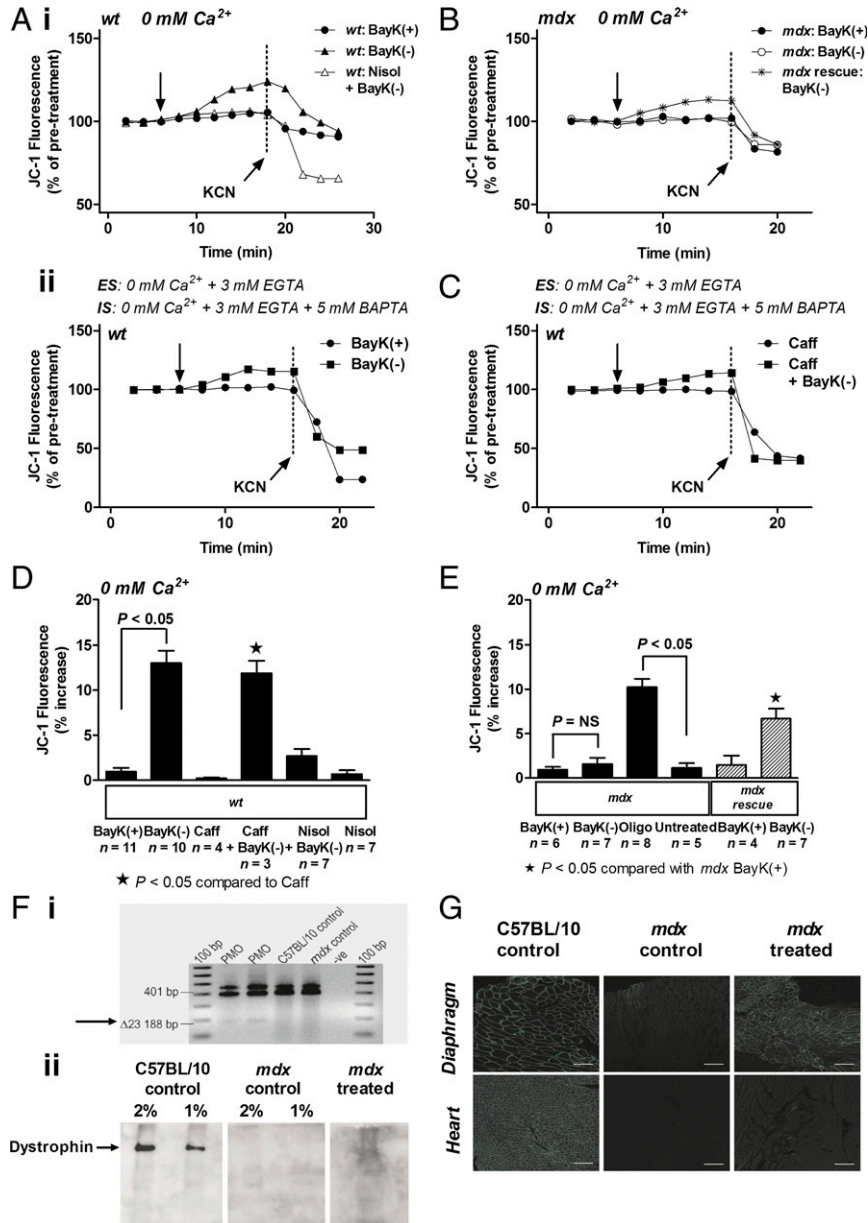

Fig. 2. Direct activation of I_{Ca-L} results in an increase in Ψ_m in *wt* but not *mdx* myocytes under calcium-free conditions. (*A*) Representative ratiometric JC-1 fluorescence recorded from *wt* myocytes before and after exposure to 10 μM BayK(+) or 10 μM BayK(-) under calcium-free conditions (0 mM Ca^{2+}) as indicated. Vertical arrow indicates when drug was added. Four micromolar KCN was added to collapse Ψ_m as indicated. ES, external solution; IS, internal solution. (*B*) Representative traces of JC-1 fluorescence recorded from *mdx* myocytes and myocytes from *mdx* mice treated with PMO ("*mdx* rescue"; see text for detail) before and after exposure to 10 μM BayK(+) or 10 μM BayK(-) under calcium-free conditions (0 mM Ca^{2+}). Vertical arrow indicates when drug was added. (*C*) Representative traces of JC-1 fluorescence recorded from *wt* myocytes before and after exposure to 2 μM caffeine (Caff) or 2 μM Caff and 10 μM BayK(-) under calcium-free conditions (0 mM Ca^{2+}) as indicated. Vertical arrow indicates when drug was added. (*D* and *E*) Mean ± SEM of increases in JC-1 fluorescence for all *wt* myocytes (*D*), and all *mdx* myocytes including myocytes from *mdx* mice treated with PMO ("*mdx* rescue") (*E*), exposed to treatments as indicated. Nisol: 10 μM nisoldipine; Oligo: 20 μM oligomycin. Oligo alone induced a robust increase in JC-1 signal in *mdx* myocytes. (*F, i*) RT-PCR performed on cardiac muscle RNA from *mdx* mice treated with PMO demonstrating exon 23 skipping (Δ23), as indicated by arrow. (*F, ii*) Immunoblot performed on cardiac muscle from C57BL/10 control mice, untreated *mdx* mice (*mdx* control), and *mdx* mice treated with PMO demonstrating presence of dystrophin (*mdx* treated), as indicated by arrow (2% and 1% dilution shown). (*G*) Immunostaining of heart and diaphragm cryosections from a C57BL/10 control mouse, untreated *mdx* mouse (*mdx* control), and *mdx* mouse treated with PMO (mouse 12-08-50) demonstrating presence of dystrophin (*mdx* treated). (Scale bars: 100 μm.)
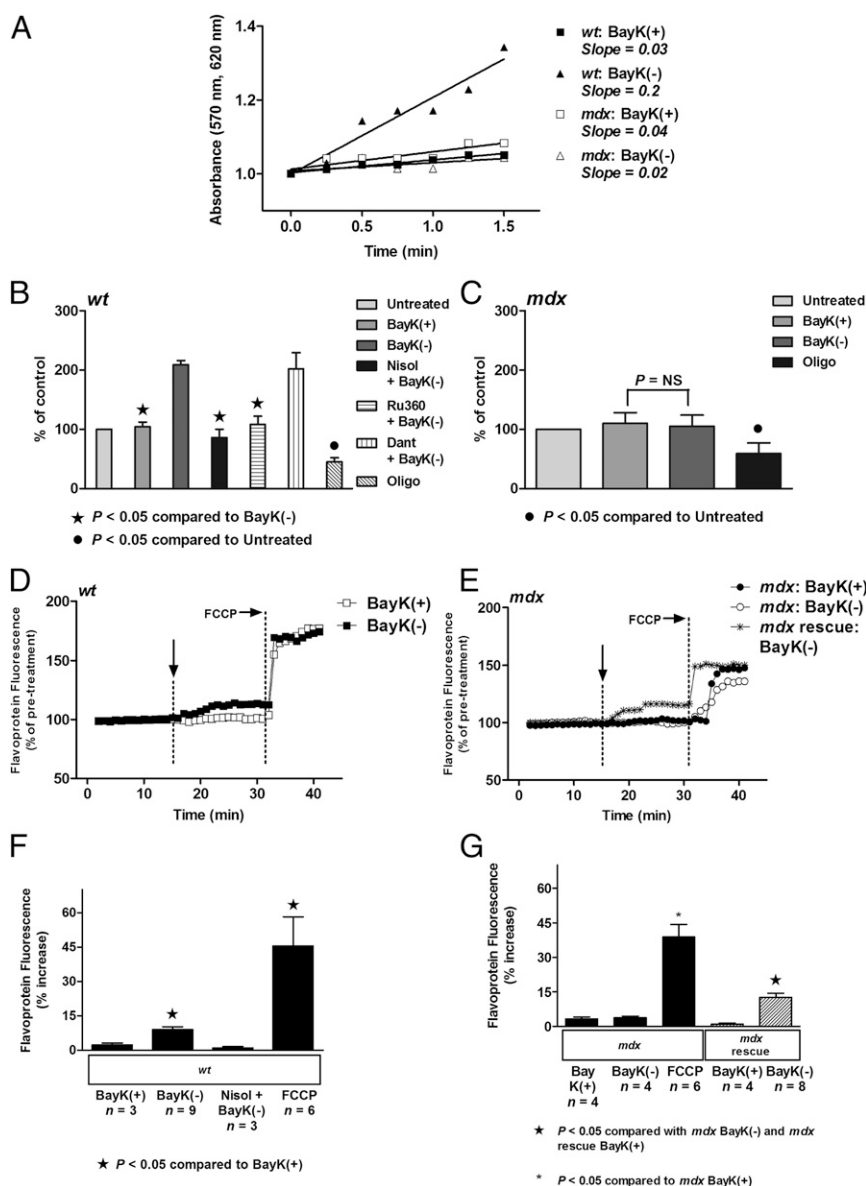
www.manaraa.com

Fig. 3. Direct activation of I_{Ca-L} results in an increase in metabolic activity and flavoprotein oxidation in *wt* but not *mdx* myocytes. (*A*) Formation of formazan measured as change in absorbance in 8-wk-old *wt* and 8-wk-old *mdx* myocytes after addition of 10 μM BayK(+) or 10 μM BayK(-). (*B* and *C*) Mean ± SEM of increases in absorbance for *wt* myocytes (*B*) and *mdx* myocytes (*C*), exposed to treatments as indicated. Dant,10 μM dantrolene; Nisol, 10 μM nisoldipine; Oligo: 20 μM oligomycin; Ru360, 10 μM Ru360. (*D* and *E*) Representative traces of flavoprotein fluorescence recorded from *wt* myocytes (*D*), and *mdx* myocytes and myocytes from *mdx* mice treated with PMO ("*mdx* rescue") (*E*), before and after exposure to 10 μM BayK(+) or 10 μM BayK(-). Vertical arrow indicates when drug was added. 10 μM FCCP was added to increase flavoprotein signal, confirming the signal was mitochondrial in origin. (*F* and *G*) Mean ± SEM of increases in flavoprotein fluorescence for all *wt* myocytes (*F*), and all *mdx* myocytes including myocytes from *mdx* mice treated with PMO ("*mdx* rescue") (*G*), exposed to treatments as indicated. FCCP, 10 μM FCCP; Nisol, 10 μM nisoldipine.

was identified as a cytoskeletal partner with I_{Ca-L}. In addition, VDAC and ANT were identified in the immunoprecipitated I_{Ca-L} protein. These data suggest I_{Ca-L} associates with the mitochondrial VDAC via cytoskeletal proteins, one of which is F-actin. The disrupted cytoskeletal architecture due to the absence of dystrophin leads to altered function between I_{Ca-L} and mitochondria.

Preventing Anion Flux Through the VDAC "Restores" the Increase in Ψ_m in mdx Myocytes. We directly blocked anion transport from the outer mitochondrial membrane with application of a peptide derived against VDAC. The VDAC peptide blocks VDAC at the mitochondrial outer membrane. In *wt* myocytes, application of the VDAC peptide increased JC-1 signal in a similar manner to

BayK(-) (Fig. 4 *C, ii* and *E*). A scrambled VDAC peptide had no effect. When the VDAC peptide was applied to *mdx* myocytes, the JC-1 signal increased significantly (Fig. 4 *D, ii* and *F*) in a similar manner to the response recorded after application of BayK(-) alone in *wt* myocytes (Fig. 4 *C, ii* and *E*). This response was also observed in myocytes incubated in calcium-free EGTA containing HBS for at least 3 h and perfused intracellularly with EGTA and BAPTA to deplete intracellular calcium stores (*wt*, Fig. 4 *C, i*; *mdx*, Fig. 4 *D, i*). These data confirm that mitochondria exhibit functional electron transport in *mdx* myocytes because a block of VDAC can increase Ψ_m. Application of VDAC restored the increase in Ψ_m in *mdx* myocytes. Taking into account that I_{Ca-L} immunoprecipitates with VDAC
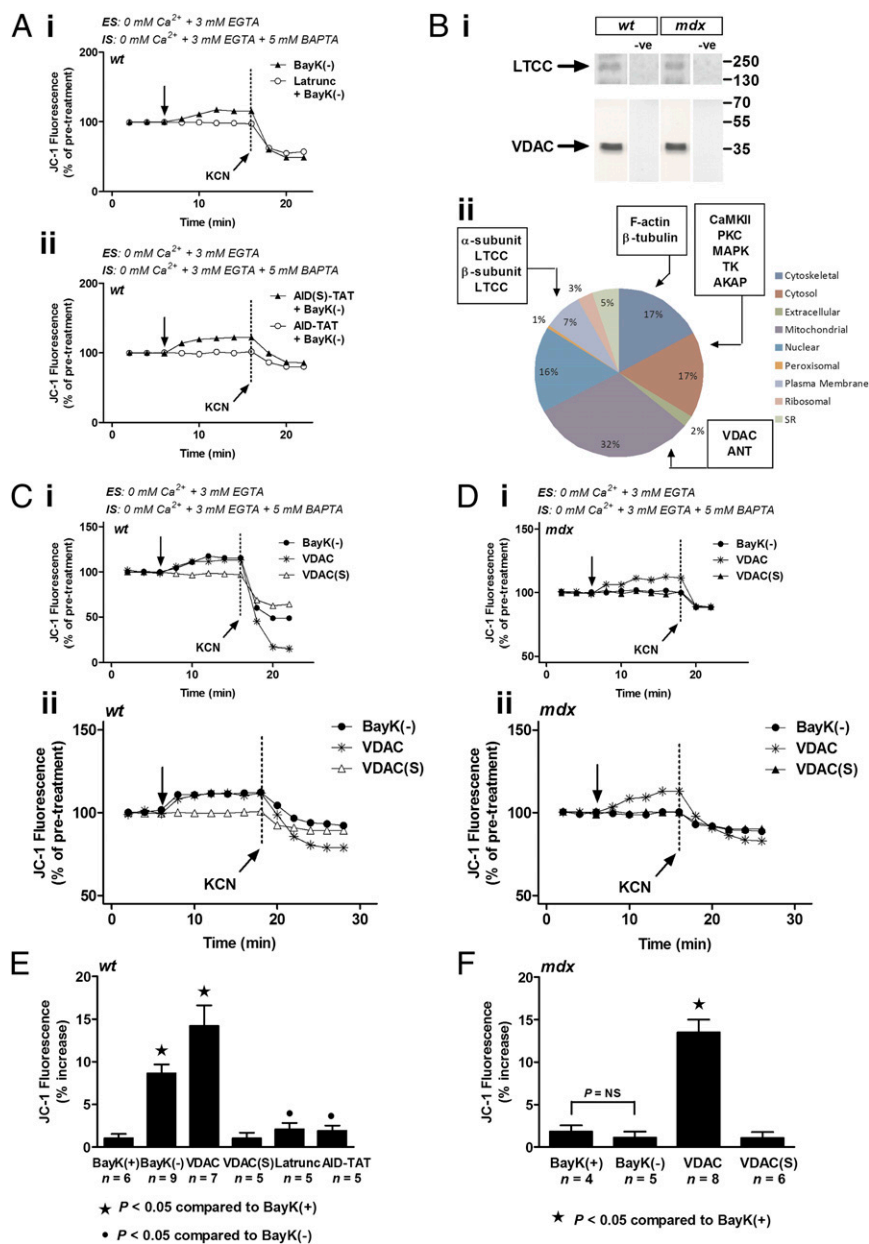
Fig. 4. VDAC coimmunoprecipitates with I_{Ca-L}, and direct block of VDAC restores the increase in Ψ_m in *mdx* myocytes. (*A*) Regulation of Ψ_m by I_{Ca-L} requires an intact cytoskeleton. Representative ratiometric JC-1 fluorescence is recorded from *wt* myocytes before and after addition of 10 μM BayK(-) in the presence or absence of 5 μM Latrunculin A (Latrunc) (*i*), or 1 μM AID(S)-TAT or 1 μM active AID-TAT peptide (*ii*), under calcium-free conditions (0 mM Ca^{2+}). Vertical arrow indicates when drug was added. Four micromolar KCN was added to collapse Ψ_m as indicated. ES, external solution; IS, internal solution. (*B*) I_{Ca-L} associates with mitochondrial VDAC via cytoskeletal proteins. (*i*) Immunoblot of 10 μg of immunoprecipitated VDAC protein from *wt* (*Left*) and *mdx* (*Right*) heart probed with anti-I_{Ca-L} antibody (*Upper*) and 10 μg immunoprecipitated I_{Ca-L} protein probed with anti-VDAC antibody (*Lower*). Negative control immunoblots were performed on 10 μg of immunoprecipitated VDAC protein from *wt* (*Left*) and *mdx* (*Right*) heart by probing with MS antibody (*Upper*), and on 10 μg of immunoprecipitated I_{Ca-L} protein from *wt* (*Left*) and *mdx* (*Right*) heart by probing with α-GOLD antibody (*Lower*). (*ii*) Mass spectrometry analysis of immunoprecipitated I_{Ca-L} protein. AKAP, A-kinase anchor protein; ANT, adenine nucleotide translocator; CaMKII, Ca^{2+}/calmodulin-dependent protein kinase II; LTCC, L-type Ca^{2+} channel; MAPK, mitogen-activated protein kinase; PKC, protein kinase C; TK, tyrosine kinase. (*C*) Application of a peptide that blocks VDAC mimics the increase in Ψ_m in *wt* myocytes. Representative ratiometric JC-1 fluorescence is recorded from *wt* myocytes before and after exposure to 10 μM BayK(-), 10 μM VDAC peptide (VDAC), or 10 μM VDAC scrambled peptide [VDAC(S)] under calcium-free (0 mM Ca^{2+}) conditions (*i*), or 2.5 mM calcium (*ii*). Vertical arrow indicates when drug was added. Four millimolar KCN was added to collapse Ψ_m as indicated. ES, external solution; IS, internal solution. (*D*) Application of a peptide that blocks VDAC restores the increase in Ψ_m in *mdx* myocytes. Representative ratiometric JC-1 fluorescence recorded from *mdx* myocytes before and after exposure to 10 μM BayK(-), 10 μM VDAC peptide (VDAC), or 10 μM VDAC scrambled peptide [VDAC(S)] under calcium-free (0 mM Ca^{2+}) conditions (*i*) or 2.5 mM calcium (*ii*). Vertical arrow indicates when drug was added. ES, external solution; IS, internal solution. (*E* and *F*) Mean ± SEM of increases in JC-1 fluorescence for all *wt* myocytes (*E*), and all *mdx* myocytes (*F*), exposed to treatments as indicated.

(Fig. 4 *B, i* and *ii*), we suggest that activation of I_{Ca-L} may increase Ψ_m in *wt* myocytes via transmission of movement of cytoskeletal proteins to VDAC.

Activation of I_{Ca-L} Increases Ψ_m in wt but Not mdx Myocytes with Established Cardiomyopathy. We isolated myocytes from 43-wk-old *mdx* hearts that had developed cardiomyopathy as assessed

on echocardiography (26) (Table S5) and examined the effect of activation of I_{Ca-L} on Ψ_m. Similar to results recorded in myocytes from 8-wk-old *mdx* mice, exposure of 43-wk-old *wt* myocytes to BayK(-) increased Ψ_m measured as changes in JC-1 signal by 9.74 ± 2.76% compared with *wt* myocytes exposed to inactive enantiomer BayK(+) (Fig. 5 *A* and *C*). The response could be attenuated with application of I_{Ca-L} antagonist nisoldipine. However, in 43-wk-old *mdx* myocytes BayK(-) could not elicit an increase in JC-1 signal (Fig. 5 *B* and *D*). Myocytes from *mdx* hearts exhibited functional electron transport because the ATP synthase blocker oligomycin induced a significant increase in JC-1 signal (Fig. 5D). To further

confirm that the signal was measuring changes in Ψ_m, we induced a collapse of Ψ_m with application of KCN.

We also examined the effect of activation of I_{Ca-L} on metabolic activity in myocytes isolated from 43-wk-old *mdx* hearts. Similar to results recorded in myocytes from 8-wk-old *wt* mice, BayK(-) elicited a significant increase in metabolic activity in myocytes from *wt* mice (Fig. 5 *E* and *F*). The response could be attenuated with application of nisoldipine or block of calcium uptake into the mitochondria (Ru360) but not with an inhibitor of the ryanodine receptor (dantrolene; Fig. 5F). However, in myocytes from 43-wk-old *mdx* hearts BayK(-) could not elicit a further increase in
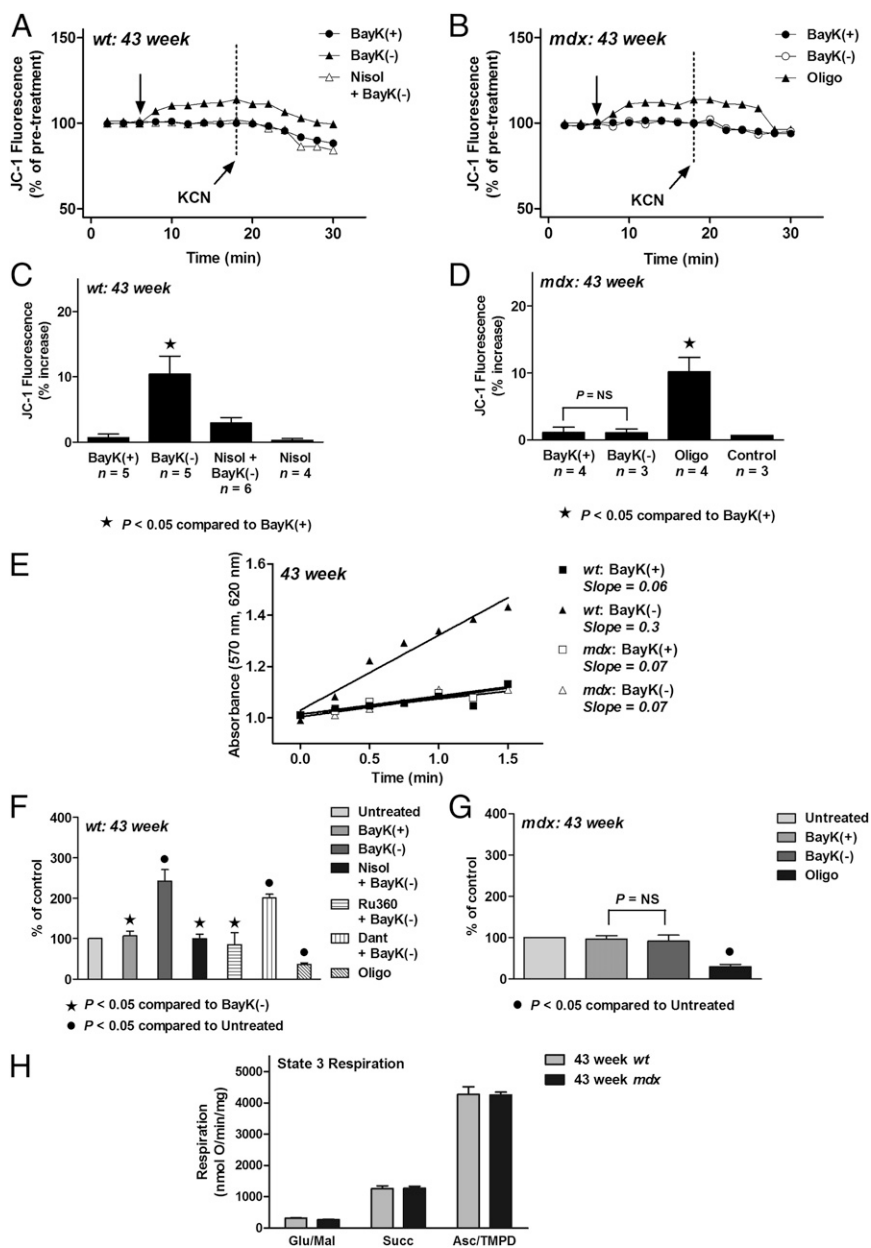

Fig. 5. Direct activation of I_{Ca-L} results in an increase in Ψ_m and metabolic activity in *wt* but not *mdx* myocytes isolated from 43-wk-old mice. (A and B) Representative ratiometric JC-1 fluorescence recorded from *wt* myocytes (*A*), and *mdx* myocytes (*B*), before and after exposure to 10 μM BayK(+) or 10 μM BayK(-). Vertical arrow indicates when drug was added. Four micromolar KCN was added to collapse Ψ_m as indicated. (C and D) Mean ± SEM of increases in JC-1 fluorescence for all *wt* (*C*) and *mdx* (*D*) myocytes exposed to treatments as indicated. Nisol, 10 μM nisoldipine; Oligo, 20 μM oligomycin. Oligo alone induced a robust increase in JC-1 signal in *mdx* myocytes. (*E*) Formation of formazan measured as change in absorbance in *wt* and *mdx* myocytes after addition of 10 μM BayK(+) or 10 μM BayK(-). (F and G) Mean ± SEM of increases in absorbance for *wt* myocytes (*F*) and *mdx* myocytes (*G*), exposed to treatments as indicated. Dant, 10 μM dantrolene; Nisol, 10 μM nisoldipine; Oligo, 20 μM oligomycin; Ru360, 10 μM Ru360. (*H*) Respiration and complex activity in mitochondria isolated from 43-wk-old *wt* hearts and 43-wk-old *mdx* hearts (see *Materials and Methods* for details).

metabolic activity (Fig. 5 *E* and *G*). Application of oligomycin caused a significant decrease in metabolic activity, indicating the cells were metabolically active (Fig. 5*G*).

To determine whether the alterations in metabolic activity in the *mdx* myocyte were specific to the mitochondria, we isolated mitochondria from hearts of 43-wk-old *mdx* mice. Respiratory complex activity and oxygen consumption were similar to that recorded in mitochondria isolated from 43-wk-old *wt* hearts (Fig. 5*H*). These data confirm that alterations in mitochondrial function occur early and persist up to the development of cardiomyopathy.

Taken together, our data suggest that the alterations in mitochondrial function depend on activation and inactivation of I_{Ca-L} in the intact cell and occur because of altered transmission of movement from I_{Ca-L} through cytoskeletal proteins to the mitochondria.

Discussion

Duchenne muscular dystrophy is a fatal X-linked disease characterized by the absence of dystrophin that is associated with cytoskeletal protein disarray, contractile dysfunction, and reduced energy production (1, 2). However, the mechanisms for altered energy metabolism are not fully understood. We have shown that activation of I_{Ca-L} alters mitochondrial function via the movement of cytoskeletal proteins (9, 12). The response depends on an intact cytoskeleton (9). In this study, we examined whether the lack of dystrophin (and associated cytoskeletal disarray; refs. 27–29) in ventricular myocytes isolated from *mdx* mice results in impaired communication between I_{Ca-L} and the mitochondria.

First, we characterized the kinetics of I_{Ca-L} current inactivation. We and others have demonstrated that disruption of the cytoskeleton alters I_{Ca-L} kinetics (11–13). We find that myocytes from *mdx* hearts exhibit a delayed inactivation of I_{Ca-L} (Fig. 1*A*). This finding is consistent with an alteration in movement of the auxiliary beta subunit of I_{Ca-L} because immobilization of the beta subunit with a peptide derived against the alpha-interacting domain also slows inactivation of the current (Fig. 1*A, Inset*). This finding is also consistent with previous studies that have demonstrated that dissociation of microtubules or depolymerization of actin alters the inactivation rate of I_{Ca-L} (5, 23, 29).

Disruption of the cytoskeleton is associated with alterations in mitochondrial function. Unlike *wt* myocytes, Ψ_m did not increase after activation of I_{Ca-L} in *mdx* myocytes (Figs. 1 and 2). In addition, metabolic activity and oxidation of flavoprotein did not increase after activation of I_{Ca-L} in *mdx* myocytes (Fig. 3). Consistent with previous studies (2), these data suggest that metabolic activity in the *mdx* myocyte is significantly different from the *wt* myocyte. Similar responses were observed in *mdx* myocytes isolated from hearts of 43-wk-old mice that had developed cardiomyopathy (Fig. 5). However, respiration was normal in mitochondria isolated from 43-wk-old mice, indicating that the responses depend on an association between I_{Ca-L} and the cytoskeleton in the intact cell (Fig. 5). Consistent with this finding, previous studies in desmin-null mice have demonstrated abnormal mitochondrial respiration in vivo, whereas the rates of maximal respiration in isolated mitochondria from desmin-null mice were similar to mitochondria isolated from *wt* mice (30). In another study, although mitochondrial distribution was normal in the hearts of 10- to 11-mo-old *mdx* mice, a lack of dystrophin was associated with impaired coupling of mitochondrial-creatine kinase to oxidative phosphorylation and altered ADP uptake by the mitochondria only in intact skinned fibers (31). Our data demonstrate that cytoskeletal disruption due to the absence of dystrophin results in the loss of regulation of mitochondrial function by I_{Ca-L} in intact *mdx* myocytes. Because I_{Ca-L} initiates contraction in the beating heart, we propose that altered communication between I_{Ca-L} and the mitochondria contributes to poor metabolic activity in the *mdx* contracting heart demonstrated as a decrease in fractional shortening on echocardiography (Table S5). Although cytosolic and mitochondrial cal-

cium are increased in the *mdx* myocyte (12, 32, 33), we propose that altered regulation of VDAC by I_{Ca-L} may contribute to the poor metabolic activity.

In this study, we demonstrate that treatment of mice with a PMO targeting dystrophin restores regulation of mitochondrial function by I_{Ca-L} in the *mdx* myocyte (Figs. 2 and 3). These data confirm that the absence of dystrophin is responsible for the lack of response of the mitochondria to activation of I_{Ca-L}. The data also demonstrate that treatment with PMOs offers a promising therapy for Duchenne muscular dystrophy cardiomyopathy.

VDAC resides in the outer mitochondrial membrane and associates with ANT that is located in the inner mitochondrial membrane (21). The VDAC/ANT complex is responsible for trafficking of ATP/ADP in and out of the mitochondria (22). VDAC and the cytoskeletal protein β-tubulin are closely associated and may play a role in regulation of mitochondrial respiration (34, 35). We examined whether I_{Ca-L} is associated with VDAC by immunoprecipitating the I_{Ca-L} protein. Immunoblot and pull-down analysis confirmed that VDAC associates with I_{Ca-L} (Fig. 4*B*). In addition, we provide functional evidence that the I_{Ca-L} communicates with VDAC. We demonstrate that preventing the opening of VDAC with application of a peptide directed toward VDAC restores the increase in JC-1 in *mdx* hearts (Fig. 4 *C* and *D*). These data to our knowledge are the first to demonstrate that I_{Ca-L} communicates with the mitochondria through an association with outer membrane mitochondrial protein VDAC via cytoskeletal proteins. We propose that communication between I_{Ca-L} and the mitochondria occurs via transmission of movement from I_{Ca-L} (during activation and inactivation of I_{Ca-L}) to mitochondrial VDAC through F-actin (Fig. 6*A*). We find that this structural and functional communication between I_{Ca-L} and the
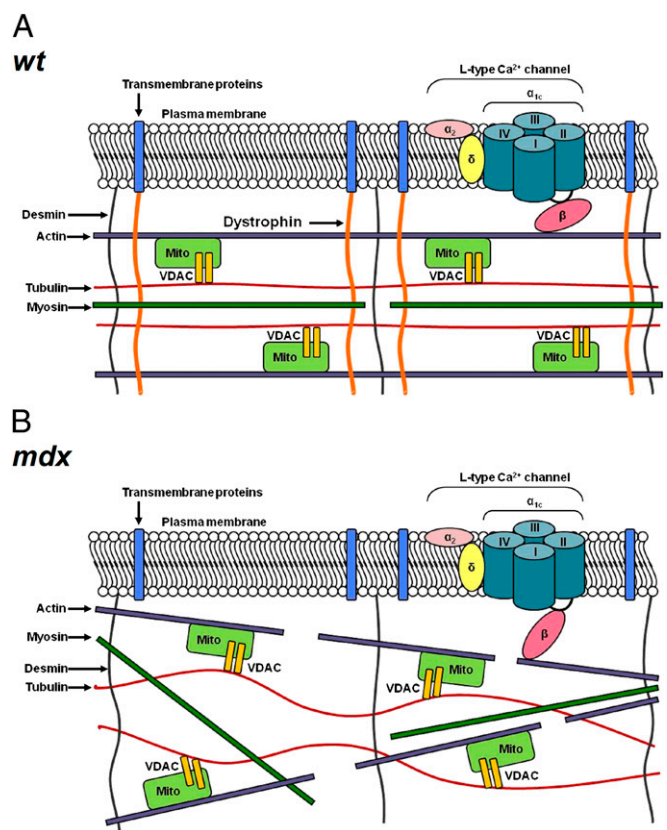

Fig. 6. Schematic representation of communication of I_{Ca-L} with the outer membrane mitochondrial protein VDAC via cytoskeletal proteins (*A*), and altered cytoskeletal network in hearts lacking dystrophin (*B*) (see text for details).

mitochondria is altered in hearts lacking dystrophin (Fig. 6B). Abnormalities occur only in the intact cell.

The VDAC/ANT complex is responsible for shuttling ATP out of the mitochondria (36). This shuttling is critical to meeting energy demands of the heart. Here, we find that the absence of dystrophin and disrupted cytoskeletal architecture in the *mdx* ventricular myocyte leads to impaired communication between I_{Ca-L} and mitochondrial VDAC. This alteration results in reduced metabolic activity in the *mdx* ventricular myocyte. These findings provide new mechanistic and functional insight into cardiomyopathy associated with Duchenne muscular dystrophy.

Materials and Methods

Isolation of Ventricular Myocytes. Myocytes were isolated from 8-wk-old and 43-wk-old male C57BL/10ScSn-Dmdmdx/Arc (*mdx*) and C57BL/10ScSnArc *wt* mice. A total number of 110 *wt* and 67 *mdx* mice were used. Four *mdx* mice were treated with PMO at 10 mg/kg per week by i.p. injection for 24 wk from 7 d of age. Cells were isolated as described (37). For full details, see *SI Materials and Methods*.

Data Acquisition for Patch-Clamp Studies. The whole-cell configuration of the patch-clamp technique was used to measure changes in I_{Ca-L} currents in intact ventricular myocytes (37, 38). Microelectrodes with tip diameters of 3–5 µm and resistances of 0.5–1.5 MΩ contained the following: 115 mM CsCl, 10 mM Hepes, 10 mM EGTA, 20 mM tetraethylammonium chloride, 5 mM MgATP, 0.1 mM Tris-GTP, 10 mM phosphocreatine, and 1 mM CaCl$_2$ (pH adjusted to 7.05 at 37 °C with CsOH). Currents were measured in extracellular modified Tyrode's solution containing the following: 140 mM NaCl, 5.4 mM CsCl, 2.5 mM CaCl$_2$, 0.5 mM MgCl$_2$, 5.5 mM Hepes, and 11 mM glucose (pH adjusted to 7.4 with NaOH). Barium currents were measured by using internal solution containing the following: 125 mM CsCl, 10 mM Hepes, 0.1 mM EGTA, 20 mM tetraethylammonium chloride, 5 mM MgATP, 0.1 mM Tris-GTP, and 10 mM phosphocreatine (pH adjusted to 7.05 at 37 °C with CsOH), and external solution containing the following: 152.5 mM tetraethylammonium chloride, 10 mM Hepes, and 10 mM BaCl$_2$ [pH adjusted to 7.4 with Ba(OH)$_2$]. Macroscopic currents were recorded by using an Axopatch 200B voltage-clamp amplifier (Molecular Devices) and an IBM compatible computer with a Digidata 1322A interface and pClamp9 software (Molecular Devices). A Ag/AgCl electrode was used to ground the bath. Once the whole-cell configuration was achieved, the holding potential was set at –80 mV. Na$^+$ channels and T-type Ca^{2+} channels were inactivated by applying a 50-ms prepulse to –30 mV immediately before each test pulse. The time course of changes in Ca^{2+} conductance were monitored by applying a 100-ms test pulse to 10 mV once every 10 s. All experiments were performed at 37 °C.

Fluorescent Studies. The fluorescent indicator 5,5′,6,6′-tetrachloro-1,1′,3,3′-tetraethylbenzimidazolylcarbocyanine iodide was used to measure Ψ_m at 37 °C as described (38). For full details, see *SI Materials and Methods*. To confirm that the JC-1 signal was indicative of Ψ_m, 4 mM KCN was added at the end of each experiment to collapse Ψ_m. For calcium-free experiments, cells were exposed to calcium-free HBS (containing 3 mM EGTA) for at least 3 h, before measuring changes in Ψ_m. In some experiments, cells were exposed to calcium-free HBS for at least 3 h and then patch-clamped with pipette solution containing the following: 115 mM CsCl, 10 mM Hepes, 5 mM BAPTA, 3 mM EGTA, 20 mM tetraethylammonium chloride, 5 mM MgATP, 0.1 mM Tris-GTP, 10 mM phosphocreatine (pH adjusted to 7.05 at 37 °C with CsOH), and 200 nM JC-1. Changes in Ψ_m were then assessed.

Flavoprotein autofluorescence was used to measure flavoprotein oxidation in intact mouse cardiac myocytes based on described methods (39). For full details, see *SI Materials and Methods*. Ten micromolar FCCP was added at the end of each experiment to achieve a maximum fluorescence value indicative of maximum flavoprotein oxidation.

RNA Preparation and RT-PCR Analysis, Immunostaining, and Immunoblot. Total RNA was extracted from the hearts, and RT-PCR was performed for analysis of exons 22–24 (Table S6). Dystrophin protein was stained on diaphragm and heart cryosections by using NCL-Dys2 and Zenon Alexafluor 488. Sections from untreated *mdx* and *wt* mice are included for comparison. All images were captured and processed by using identical parameters (18, 40). Dystrophin protein was assessed on immunoblot as described (40, 41). For full details, see *SI Materials and Methods*.

Yellow Tetrazolium Salt Assay. The rate of cleavage of yellow tetrazolium salt to purple formazan crystals by the mitochondrial electron transport chain was measured spectrophotometrically at 570 nm with a reference wavelength of 620 nm at 37 °C as described (9). Each *n* represents number of animals used in each treatment group for the assay. For full details, see *SI Materials and Methods*.

Immunoprecipitation of I_{Ca-L} and VDAC Protein and Immunoblot. Membrane fractions were prepared from crude heart homogenates as described (42). Immunoprecipitation and immunoblot were performed as described (25, 42), using either anti-I_{Ca-L} antibody (ACC-004; Alomone Labs) or anti-porin antibody (MSA03; MitoSciences). Immunoprecipitation was performed by using PureProteome Protein G Magnetic Beads (Millipore). Rabbit polyclonal antibody raised in house against a gold N-heterocyclic carbene compound (α-GOLD) or serum from pooled BALB/c and C57BL/6 mice (MS) were used as negative controls. For full details, see *SI Materials and Methods*.

Mass Spectrometry Analysis of Immunoprecipitated I_{Ca-L} Protein. Digest peptides were separated by nano-LC using an Ultimate 3000 HPLC and auto-sampler system (Dionex) at The Bioanalytical Mass Spectrometry Facility, University of New South Wales, Sydney. Samples were analyzed by using an Orbitrap Velos (Thermo Electron) mass spectrometer. For full details, see *SI Materials and Methods*.

Mitochondrial Respiration Studies. Mitochondrial respiration was measured in mitochondria isolated from three pooled wt mouse hearts and from three pooled mdx mouse hearts by using a OROBOROS high resolution respirometer thermostatically maintained at 37 °C as described (43). For full details, see *SI Materials and Methods*.

Statistical Analysis. Results are reported as mean ± SEM. Statistical comparisons of responses between unpaired data were made by using the Student *t* test or between groups of cells by using one-way ANOVA and the Tukey's post hoc test (GraphPad Prism version 5.04).

1. Finsterer J, Stöllberger C (2003) The heart in human dystrophinopathies. *Cardiology* 99(1):1–19.
2. Khairallah M, et al. (2007) Metabolic and signaling alterations in dystrophin-deficient hearts precede overt cardiomyopathy. *J Mol Cell Cardiol* 43(2):119–129.
3. Tokuyasu KT, Dutton AH, Singer SJ (1983) Immunoelectron microscopic studies of desmin (skeletin) localization and intermediate filament organization in chicken cardiac muscle. *J Cell Biol* 96(6):1736–1742.
4. Thornell LE, et al. (1985) Intermediate filament and associated proteins in heart Purkinje fibers: A membrane-myofibril anchored cytoskeletal system. *Ann N Y Acad Sci* 455:213–240.
5. Lader AS, Kwiatkowski DJ, Cantiello HF (1999) Role of gelsolin in the actin filament regulation of cardiac L-type calcium channels. *Am J Physiol* 277(6 Pt 1):C1277–C1283.
6. Hohaus A, et al. (2002) The carboxyl-terminal region of ahnak provides a link between cardiac L-type Ca2+ channels and the actin-based cytoskeleton. *FASEB J* 16(10):1205–1216.
7. Rueckschloss U, Isenberg G (2001) Cytochalasin D reduces Ca^{2+} currents via cofilin-activated depolymerization of F-actin in guinea-pig cardiomyocytes. *J Physiol* 537(Pt 2):363–370.
8. Nakamura M, Sunagawa M, Kosugi T, Sperelakis N (2000) Actin filament disruption inhibits L-type Ca($^{2+}$) channel current in cultured vascular smooth muscle cells. *Am J Physiol Cell Physiol* 279(2):C480–C487.
9. Viola HM, Arthur PG, Hool LC (2009) Evidence for regulation of mitochondrial function by the L-type Ca^{2+} channel in ventricular myocytes. *J Mol Cell Cardiol* 46(6):1016–1026.
10. Viola HM, Hool LC (2010) Cross-talk between L-type Ca2+ channels and mitochondria. *Clin Exp Pharmacol Physiol* 37(2):229–235.
11. Woolf PJ, et al. (2006) Alterations in dihydropyridine receptors in dystrophin-deficient cardiac muscle. *Am J Physiol Heart Circ Physiol* 290(6):H2439–H2445.
12. Viola HM, Davies SM, Filipovska A, Hool LC (2013) L-type Ca(2+) channel contributes to alterations in mitochondrial calcium handling in the mdx ventricular myocyte. *Am J Physiol Heart Circ Physiol* 304(6):H767–H775.

Viola et al.

www.manaraa.com

13. Koenig X, et al. (2011) Voltage-gated ion channel dysfunction precedes cardiomyopathy development in the dystrophic heart. *PLoS ONE* 6(5):e20300.

14. Pragnell M, et al. (1994) Calcium channel β-subunit binds to a conserved motif in the I-II cytoplasmic linker of the α$_1$-subunit. *Nature* 368(6466):67–70.

15. Kobrinsky E, et al. (2005) Differential role of the α$_{1C}$ subunit tails in regulation of the Ca$_v$1.2 channel by membrane potential, β subunits, and Ca^{2+} ions. *J Biol Chem* 280(13):12474–12485.

16. Territo PR, Mootha VK, French SA, Balaban RS (2000) Ca($^{2+}$) activation of heart mitochondrial oxidative phosphorylation: Role of the F$_{(0)}$/F$_{(1)}$-ATPase. *Am J Physiol Cell Physiol* 278(2):C423–C435.

17. Balaban RS (2002) Cardiac energy metabolism homeostasis: Role of cytosolic calcium. *J Mol Cell Cardiol* 34(10):1259–1271.

18. Gebski BL, Mann CJ, Fletcher S, Wilton SD (2003) Morpholino antisense oligonucleotide induced dystrophin exon 23 skipping in mdx mouse muscle. *Hum Mol Genet* 12(15):1801–1811.

19. Cirak S, et al. (2011) Exon skipping and dystrophin restoration in patients with Duchenne muscular dystrophy after systemic phosphorodiamidate morpholino oligomer treatment: An open-label, phase 2, dose-escalation study. *Lancet* 378(9791):595–605.

20. Kinali M, et al. (2009) Local restoration of dystrophin expression with the morpholino oligomer AVI-4658 in Duchenne muscular dystrophy: A single-blind, placebo-controlled, dose-escalation, proof-of-concept study. *Lancet Neurol* 8(10):918–928.

21. Crompton M, Virji S, Ward JM (1998) Cyclophilin-D binds strongly to complexes of the voltage-dependent anion channel and the adenine nucleotide translocase to form the permeability transition pore. *Eur J Biochem* 258(2):729–735.

22. Rostovtseva T, Colombini M (1996) ATP flux is controlled by a voltage-gated channel from the mitochondrial outer membrane. *J Biol Chem* 271(45):28006–28008.

23. Galli A, DeFelice LJ (1994) Inactivation of L-type Ca channels in embryonic chick ventricle cells: Dependence on the cytoskeletal agents colchicine and taxol. *Biophys J* 67(6):2296–2304.

24. Hao LY, Xu JJ, Minobe E, Kameyama A, Kameyama M (2008) Calmodulin kinase II activation is required for the maintenance of basal activity of L-type Ca2+ channels in guinea-pig ventricular myocytes. *J Pharmacol Sci* 108(3):290–300.

25. Nichols CB, et al. (2010) Sympathetic stimulation of adult cardiomyocytes requires association of AKAP5 with a subpopulation of L-type calcium channels. *Circ Res* 107(6):747–756.

26. Spurney CF, et al. (2008) Dystrophin-deficient cardiomyopathy in mouse: Expression of Nox4 and Lox are associated with fibrosis and altered functional parameters in the heart. *Neuromuscul Disord* 18(5):371–381.

27. Bloch RJ, et al. (2002) Costameres: Repeating structures at the sarcolemma of skeletal muscle. *Clin Orthop Relat Res* (403, Suppl):S203–S210.

28. Quinlan JG, et al. (2004) Evolution of the mdx mouse cardiomyopathy: Physiological and morphological findings. *Neuromuscul Disord* 14(8-9):491–496.

29. Sadeghi A, Doyle AD, Johnson BD (2002) Regulation of the cardiac L-type Ca^{2+} channel by the actin-binding proteins α-actinin and dystrophin. *Am J Physiol Cell Physiol* 282(6):C1502–C1511.

30. Capetanaki Y (2002) Desmin cytoskeleton: A potential regulator of muscle mitochondrial behavior and function. *Trends Cardiovasc Med* 12(8):339–348.

31. Braun U, et al. (2001) Lack of dystrophin is associated with altered integration of the mitochondria and ATPases in slow-twitch muscle cells of MDX mice. *Biochim Biophys Acta* 1505(2-3):258–270.

32. Jung C, Martins AS, Niggli E, Shirokova N (2008) Dystrophic cardiomyopathy: Amplification of cellular damage by Ca^{2+} signalling and reactive oxygen species-generating pathways. *Cardiovasc Res* 77(4):766–773.

33. Allen DG, Gervasio OL, Yeung EW, Whitehead NP (2010) Calcium and the damage pathways in muscular dystrophy. *Can J Physiol Pharmacol* 88(2):83–91.

34. Rostovtseva TK, et al. (2008) Tubulin binding blocks mitochondrial voltage-dependent anion channel and regulates respiration. *Proc Natl Acad Sci USA* 105(48):18746–18751.

35. Kay L, et al. (1997) Study of regulation of mitochondrial respiration in vivo. An analysis of influence of ADP diffusion and possible role of cytoskeleton. *Biochim Biophys Acta* 1322(1):41–59.

36. Shoshan-Barmatz V, Ben-Hail D (2012) VDAC, a multi-functional mitochondrial protein as a pharmacological target. *Mitochondrion* 12(1):24–34.

37. Hool LC (2000) Hypoxia increases the sensitivity of the L-type Ca(2+) current to beta-adrenergic receptor stimulation via a C2 region-containing protein kinase C isoform. *Circ Res* 87(12):1164–1171.

38. Viola HM, Arthur PG, Hool LC (2007) Transient exposure to hydrogen peroxide causes an increase in mitochondria-derived superoxide as a result of sustained alteration in L-type Ca^{2+} channel function in the absence of apoptosis in ventricular myocytes. *Circ Res* 100(7):1036–1044.

39. Yaniv Y, et al. (2011) Ca2+-regulated-cAMP/PKA signaling in cardiac pacemaker cells links ATP supply to demand. *J Mol Cell Cardiol* 51(5):740–748.

40. Mann CJ, et al. (2001) Antisense-induced exon skipping and synthesis of dystrophin in the mdx mouse. *Proc Natl Acad Sci USA* 98(1):42–47.

41. Mann CJ, Honeyman K, McClorey G, Fletcher S, Wilton SD (2002) Improved antisense oligonucleotide induced exon skipping in the mdx mouse model of muscular dystrophy. *J Gene Med* 4(6):644–654.

42. Tang H, Viola HM, Filipovska A, Hool LC (2011) Ca(v)1.2 calcium channel is glutathionylated during oxidative stress in guinea pig and ischemic human heart. *Free Radic Biol Med* 51(8):1501–1511.

43. Davies SM, Poljak A, Duncan MW, Smythe GA, Murphy MP (2001) Measurements of protein carbonyls, ortho- and meta-tyrosine and oxidative phosphorylation complex activity in mitochondria from young and old rats. *Free Radic Biol Med* 31(2):181–190.

www.manaraa.com